Physica A 391 (2012) 1009–1019

Contents lists available at SciVerse ScienceDirect

Physica A

journal homepage: www.elsevier.com/locate/physa

A practically unconditionally gradient stable scheme for the *N*-component Cahn–Hilliard system

Hyun Geun Lee, Jeong-Whan Choi, Junseok Kim *

Department of Mathematics, Korea University, Seoul 136-701, Republic of Korea

ARTICLE INFO

Article history:
Received 1 August 2011
Available online 25 November 2011

Keywords:
N-component Cahn–Hilliard system
Practically unconditionally gradient stable
Nonlinear multigrid
Phase separation
Finite difference

ABSTRACT

We present a practically unconditionally gradient stable conservative nonlinear numerical scheme for the *N*-component Cahn–Hilliard system modeling the phase separation of an *N*-component mixture. The scheme is based on a nonlinear splitting method and is solved by an efficient and accurate nonlinear multigrid method. The scheme allows us to convert the *N*-component Cahn–Hilliard system into a system of $N-1$ binary Cahn–Hilliard equations and significantly reduces the required computer memory and CPU time. We observe that our numerical solutions are consistent with the linear stability analysis results. We also demonstrate the efficiency of the proposed scheme with various numerical experiments.

1. Introduction

The Cahn–Hilliard (CH) equation is the prototypical continuum model of phase separation in a binary alloy. It was originally derived by Cahn and Hilliard [1] to describe spinodal decomposition and has been widely adopted to model many other physical phenomena such as contact angle and wetting problem [2–4], gravity and capillary waves [5,6], mixing [7], pinchoff of liquid–liquid jets [8,9], Rayleigh–Taylor instability [10–13], solid tumor growth [14–16], thermocapillary flow [17,18], and vesicle dynamics [19].

Most of the technologically important alloys are multi-component systems exhibiting multiple phases in their microstructures. Moreover, one or more of these phases are formed as a result of phase transformations induced during processing. Since performance of these multi-component alloys depends crucially on the morphology of the phases, a fundamental understanding of the kinetics of phase transformations is important for controlling the microstructures of these multi-phase alloys [20].

The generalization of the CH equation to multi-component systems first appeared in the literature of De Fontaine [21] and Morral and Cahn [22]. Hoyt [23] extended the CH continuum theory of nucleation to multi-component solutions. Elliott and Luckhaus [24] gave a global existence result under constant mobility and specific assumptions. Eyre [25] studied differences between multi-component and binary alloys and discussed the equilibrium and dynamic behavior of multi-component systems. Elliot and Garcke [26] proved a global existence for multi-component systems when the mobility matrix depends on a concentration. Maier-Paape et al. [27] explained the initial-stage phase separation process in multi-component CH systems through spinodal decomposition.

There are many numerical studies with the binary CH equation [4,9,13,28–40], ternary [20,28,41–52], and quaternary [53–57] CH systems. One of the main difficulties in solving the CH system numerically is that the system is fourth-order in space which makes difference stencils very large and introduces a severe time step restriction for stability, i.e., $\Delta t \sim (\Delta x)^4$

* Corresponding author. Tel.: +82 2 3290 3077; fax: +82 2 929 8562.
E-mail addresses: cfdkim@korea.ac.kr, junseok_kim@yahoo.com (J. Kim).
URL: http://math.korea.ac.kr/~cfdkim/ (J. Kim).

0378-4371/$ – see front matter © 2011 Elsevier B.V. All rights reserved.
doi:10.1016/j.physa.2011.11.032

for explicit methods. And there is a nonlinearity at the lower order spatial derivatives which can also contribute to numerical stability. Copetti [43] considered an explicit finite element approximation of a model for phase separation in a ternary mixture and took $\Delta x = 1.0$ and $\Delta t = 0.01$ in numerical experiments. In [20], Bhattacharyya and Abinandanan used a semi-implicit Fourier spectral method for solving the ternary CH equations. They treated the linear fourth-order terms implicitly and the non-linear terms explicitly and simulations were carried out using $\Delta x = 1.0$ and $\Delta t = 0.05$. Ma [44] performed numerical simulation of the phase separation kinetics in ternary mixtures with different interfacial properties by means of the cell dynamics approach and in the literature Δx and Δt were both set to be unity. In [41], Δx and Δt were also both set to be unity. Kim and Lowengrub [46] developed a stable, conservative, and second-order accurate fully implicit discretization of the ternary CH system. The authors used a nonlinear multigrid method to efficiently solve the discrete ternary CH system at the implicit time-level and a uniform time step $\Delta t \leq 0.25\Delta x$ for a uniform mesh size Δx. Boyer and Lapuerta [48] used the implicit Galerkin finite elements method with $\Delta x = 8.33 \times 10^{-4}$ and $\Delta t = 0.001$ to solve the ternary CH system.

In numerous papers, there are stability restrictions on the time step which cause huge computational costs and make the calculation very inefficient. Therefore we need a scheme that allows the use of a sufficiently large time step without the technical limitations. But, though such an algorithm allows the use of a sufficiently large time step, it seems to be less attractive, because we need to invert an $(N-1)\times(N-1)$ matrix to obtain the solution of the N-component CH system (except for the explicit method) and the matrix inversion becomes more and more complicated for increasing N. This problem was shown in previous papers. The authors in [54] developed a nonlinear multigrid method to efficiently solve the discrete N-component CH system at the implicit time level, but an iteration step for the nonlinear multigrid method consists of a $2(N-1)\times 2(N-1)$ matrix inversion.

In the literature [58–62], to overcome this problem, a variety of numerical approaches have been developed for a large number of components. These approaches can significantly reduce the required computer memory and CPU time, but such approaches are limited to the Allen–Cahn system. Adaptive mesh refinement (AMR) [16,33,38,63,64] has been used in the CH simulations to increase computational efficiency, but implementation of AMR could be difficult and, in general, AMR is employed only by a small number of components.

In this paper, we present a practically unconditionally gradient stable conservative numerical method for solving the CH system representing a model for phase separation in an N-component mixture. This method allows us to solve the N-component CH system in a decoupled way and significantly reduces the CPU time and memory requirements. We emphasize that while the method will allow us to take arbitrarily large time steps, the accuracy of the numerical solution depends on choosing a small enough time step to resolve the dynamics [65].

This paper is organized as follows. In Section 2, we briefly review the governing equations for phase separation in the N-component CH system. In Section 3, we consider a nonlinear splitting finite difference scheme for the N-component CH system. We present numerical experiments in Section 4. Finally, conclusions are drawn in Section 5.

2. Governing equations

We consider the evolution of the N-component CH system on a domain $\Omega \subset \mathbb{R}^d$, $d = 1, 2, 3$. Let $\mathbf{c} = (c_1, \ldots, c_N)$ be the phase variables (i.e., the mole fractions of different components). Clearly the total mole fractions must sum to 1, i.e.,

$$c_1 + \cdots + c_N = 1,$$

so that, admissible states will belong to the Gibbs N-simplex

$$G := \left\{ \mathbf{c} \in \mathbb{R}^N \,\middle|\, \sum_{i=1}^{N} c_i = 1, 0 \leq c_i \leq 1 \right\}. \tag{1}$$

Without loss of generality, we postulate that the free energy can be written as follows:

$$\mathcal{F}(\mathbf{c}) = \int_{\Omega} \left(F(\mathbf{c}) + \frac{\epsilon^2}{2} \sum_{i=1}^{N} |\nabla c_i|^2 \right) \mathrm{d}\mathbf{x}, \tag{2}$$

where $F(\mathbf{c}) = 0.25 \sum_{i=1}^{N} c_i^2 (1 - c_i)^2$ and $\epsilon > 0$ is the gradient energy coefficient. The natural boundary condition for the N-component CH system is the zero Neumann boundary condition:

$$\nabla c_i \cdot \mathbf{n} = 0 \quad \text{on } \partial\Omega, \tag{3}$$

where $\mathbf{n}$ is the unit normal vector to $\partial\Omega$.

The time evolution of $\mathbf{c}$ is governed by the gradient of the energy with respect to the $\dot{H}^{-1}$ inner product under the additional constraint (1). This constraint has to hold everywhere at any time. In order to ensure this last constraint, we use a variable Lagrangian multiplier $\beta(\mathbf{c})$ [66]. The time dependence of c_i is given by the following CH equation:

$$\frac{\partial c_i}{\partial t} = M \Delta \mu_i, \tag{4}$$

$$\mu_i = f(c_i) - \epsilon^2 \Delta c_i + \beta(\mathbf{c}), \quad \text{for } i = 1, \ldots, N, \tag{5}$$

where M is a mobility, $f(c) = c(c - 0.5)(c - 1)$, and $\beta(\mathbf{c}) = -\frac{1}{N} \sum_{i=1}^{N} f(c_i)$. We take $M \equiv 1$ for convenience.

The mass conserving boundary condition for the N-component CH system is

$$\nabla\mu_i \cdot \mathbf{n} = 0 \quad \text{on } \partial\Omega. \tag{6}$$

We differentiate the energy $\mathcal{F}$ and the total mass of each phase, $\int_\Omega c_i \, d\mathbf{x}$, to get

$$\frac{d}{dt}\mathcal{F}(t) = -M \int_\Omega \sum_{i=1}^{N} |\nabla\mu_i|^2 \, d\mathbf{x} \le 0 \tag{7}$$

and

$$\frac{d}{dt}\int_\Omega c_i \, d\mathbf{x} = 0, \tag{8}$$

where we used the mass conserving boundary condition (6). For a more detailed description of derivations of (7) and (8), please refer to Ref. [54]. Therefore, the total energy is non-increasing in time and the total mass of each phase is conserved. That is

$$\mathcal{F}(t) \le \mathcal{F}(0) \quad \text{and} \quad \int_\Omega c_i(\mathbf{x}, t) \, d\mathbf{x} = \int_\Omega c_i(\mathbf{x}, 0) \, d\mathbf{x} \quad \text{for } i = 1, \ldots, N.$$

3. Numerical solution

The numerical solution of the N-component CH system uses a second-order accurate spatial discretization and a nonlinear splitting time stepping method. For simplicity and clarity of exposition, we will present the numerical method in 2D, but the extension to 3D is straightforward. Note that we only need to solve equations with $c_1, c_2, \ldots, c_{N-1}$ since $c_N = 1 - c_1 - c_2 - \cdots - c_{N-1}$ for the N-component CH system. Let $\mathbf{c} = (c_1, c_2, \ldots, c_{N-1})$ and $\boldsymbol{\mu} = (\mu_1, \mu_2, \ldots, \mu_{N-1})$.

3.1. Discretization

Let $\Omega = (a, b) \times (c, d)$ be the computational domain in 2D, N_x and N_y be positive even integers, $h = (b - a)/N_x$ be the uniform mesh size, and $\Omega_h = \{(x_i, y_j) : x_i = (i - 0.5)h, y_j = (j - 0.5)h, 1 \le i \le N_x, 1 \le j \le N_y\}$ be the set of cell-centers.

Let $\mathbf{c}_{ij}$ and $\boldsymbol{\mu}_{ij}$ be approximations of $\mathbf{c}(x_i, y_j)$ and $\boldsymbol{\mu}(x_i, y_j)$. We first implement the zero Neumann boundary condition (3) and (6) by requiring that

$$D_x\mathbf{c}_{\frac{1}{2},j} = D_x\mathbf{c}_{N_x+\frac{1}{2},j} = D_y\mathbf{c}_{i,\frac{1}{2}} = D_y\mathbf{c}_{i,N_y+\frac{1}{2}} = \mathbf{0},$$
$$D_x\boldsymbol{\mu}_{\frac{1}{2},j} = D_x\boldsymbol{\mu}_{N_x+\frac{1}{2},j} = D_y\boldsymbol{\mu}_{i,\frac{1}{2}} = D_y\boldsymbol{\mu}_{i,N_y+\frac{1}{2}} = \mathbf{0},$$

where the discrete differentiation operators are

$$D_x\mathbf{c}_{i+\frac{1}{2},j} = (\mathbf{c}_{i+1,j} - \mathbf{c}_{ij})/h \quad \text{and} \quad D_y\mathbf{c}_{i,j+\frac{1}{2}} = (\mathbf{c}_{i,j+1} - \mathbf{c}_{ij})/h.$$

We then define the discrete Laplacian by

$$\Delta_h\mathbf{c}_{ij} = \left(D_x\mathbf{c}_{i+\frac{1}{2},j} - D_x\mathbf{c}_{i-\frac{1}{2},j} + D_y\mathbf{c}_{i,j+\frac{1}{2}} - D_y\mathbf{c}_{i,j-\frac{1}{2}}\right)/h$$

and the discrete L^2 inner product by

$$(\mathbf{c}, \mathbf{d})_h = h^2 \sum_{i=1}^{N_x}\sum_{j=1}^{N_y}(c_{1ij}d_{1ij} + c_{2ij}d_{2ij} + \cdots + c_{N-1ij}d_{N-1ij}). \tag{9}$$

We also define a discrete norm associated with (9) as

$$\|\mathbf{c}\|^2 = (\mathbf{c}, \mathbf{c})_h.$$

We define $\mathbf{f}(\mathbf{c})$ and $\mathbf{1}$ to $\mathbf{f}(\mathbf{c}) = (f(c_1), f(c_2), \ldots, f(c_{N-1}))$ and $\mathbf{1} = (1, 1, \ldots, 1) \in \mathbb{R}^{N-1}$. We discretize Eqs. (4) and (5) in time by a nonlinear splitting algorithm:

$$\frac{\mathbf{c}_{ij}^{n+1} - \mathbf{c}_{ij}^{n}}{\Delta t} = \Delta_h\boldsymbol{\nu}_{ij}^{n+1} + \Delta_h\left(\beta(\mathbf{c}_{ij}^{n})\mathbf{1} - \frac{1}{4}\mathbf{c}_{ij}^{n}\right), \tag{10}$$

$$\boldsymbol{\nu}_{ij}^{n+1} = \boldsymbol{\varphi}(\mathbf{c}_{ij}^{n+1}) - \epsilon^2\Delta_h\mathbf{c}_{ij}^{n+1}, \tag{11}$$

where the nonlinear function $\boldsymbol{\varphi}(\mathbf{c}) = (\varphi_1(\mathbf{c}), \varphi_2(\mathbf{c}), \ldots, \varphi_{N-1}(\mathbf{c})) = \mathbf{f}(\mathbf{c}) + \mathbf{c}/4$.

Table 1
The values of the maximum time step guaranteeing the stability of each scheme.

Case	32×32	64×64	128×128	256×256
EE	7.6×10^{-5}	1.9×10^{-5}	4.7×10^{-6}	1.1×10^{-6}
SIE	2.9×10^{-2}	7.9×10^{-3}	1.3×10^{-3}	4.3×10^{-4}
IE	3.2×10^{-2}	7.8×10^{-3}	1.7×10^{-3}	4.4×10^{-4}
CN	2.0×10^{-2}	5.0×10^{-3}	1.1×10^{-3}	2.8×10^{-4}
NS	∞	∞	∞	∞

In Eq. (10), the variable Lagrangian multiplier $\beta(\mathbf{c})$ is determined by the solutions at time level n. By treating $\beta(\mathbf{c})$ explicitly, there is no relation between the solutions at time level $n+1$. Thus the N-component CH system can be solved in a decoupled way, i.e.,

$$\frac{c_{k,ij}^{n+1} - c_{k,ij}^{n}}{\Delta t} = \Delta_h \nu_{k,ij}^{n+1} + \Delta_h \left(\beta(\mathbf{c}_{ij}^{n}) - \frac{1}{4} c_{k,ij}^{n} \right),$$
$$\nu_{k,ij}^{n+1} = \varphi(c_{k,ij}^{n+1}) - \epsilon^2 \Delta_h c_{k,ij}^{n+1}, \quad \text{for } k = 1, 2, \ldots, N-1.$$

This means that we only solve the binary CH equation $N-1$ times to solve the N-component CH system. The above discrete system is solved by a nonlinear multigrid method [67].

4. Numerical experiments

4.1. The stability of the proposed scheme

We investigate the stability of five different schemes for the quaternary CH system: the explicit Euler's (EE), semi-implicit Euler's (SIE), implicit Euler's (IE), Crank–Nicolson (CN), and nonlinear splitting (NS). For dissipative dynamics such as the CH system, a discrete time stepping algorithm is defined to be gradient stable if the free energy is nonincreasing, $\mathcal{F}(\mathbf{c}^{n+1}) \leq \mathcal{F}(\mathbf{c}^{n})$, for each n. Define $\Delta t_{\max}$ as the largest possible time step which allows stable numerical computation. In other words, if the time step is larger than $\Delta t_{\max}$, then the algorithm is not gradient stable. To measure $\Delta t_{\max}$ for each scheme, we perform a number of simulations for a sample initial problem on a set of increasingly finer grids. The initial conditions are

$$c_1(x, y, 0) = 0.25 + 0.1\text{rand}(\,),$$
$$c_2(x, y, 0) = 0.25 + 0.1\text{rand}(\,),$$
$$c_3(x, y, 0) = 0.25 + 0.1\text{rand}(\,)$$

on a domain $\Omega = (0, 1) \times (0, 1)$. Here, rand( ) is a random number between -1 and 1. The numerical solutions are computed on the uniform grids, $h = 1/2^n$ for $n = 5, 6, 7$, and 8. For each case, $\epsilon = 0.64h$ is used. The values of $\Delta t_{\max}$ with different schemes are listed in Table 1. From the results, we observe that EE, SIE, IE, and CN schemes are not gradient stable when we use the time step larger than $\Delta t_{\max}$ (see Fig. 1). However, our proposed scheme (NS) is gradient stable for time steps of any size, i.e., the scheme is practically unconditionally gradient stable.

4.2. Linear stability analysis

In this section, we study the short-time behavior of a quaternary mixture. The partial differential equations (4) and (5) we wish to solve may be written as

$$\frac{\partial \mathbf{c}(x, t)}{\partial t} = \Delta \left(\psi(\mathbf{c}) - \epsilon^2 \Delta \mathbf{c} \right), \quad \text{for } (x, t) \in \Omega \times (0, T], \tag{12}$$

where $\psi(\mathbf{c}) = \mathbf{f}(\mathbf{c}) + \beta(\mathbf{c})\mathbf{1}$. Let the mean concentration take the form $\mathbf{m} = (m_1, m_2, m_3)$. We seek a solution of the form

$$\mathbf{c}(x, t) = \mathbf{m} + \sum_{k=1}^{\infty} \cos(k\pi x)(\alpha_k(t), \beta_k(t), \gamma_k(t)), \tag{13}$$

where $|\alpha_k(t)|$, $|\beta_k(t)|$, and $|\gamma_k(t)| \ll 1$. After linearizing $\psi(\mathbf{c})$ about $\mathbf{m}$, we have

$$\psi(\mathbf{c}) \approx \psi(\mathbf{m}) + (\mathbf{c} - \mathbf{m}) \begin{pmatrix} \partial_{c_1}\psi_1(\mathbf{m}) & \partial_{c_1}\psi_2(\mathbf{m}) & \partial_{c_1}\psi_3(\mathbf{m}) \\ \partial_{c_2}\psi_1(\mathbf{m}) & \partial_{c_2}\psi_2(\mathbf{m}) & \partial_{c_2}\psi_3(\mathbf{m}) \\ \partial_{c_3}\psi_1(\mathbf{m}) & \partial_{c_3}\psi_2(\mathbf{m}) & \partial_{c_3}\psi_3(\mathbf{m}) \end{pmatrix}. \tag{14}$$

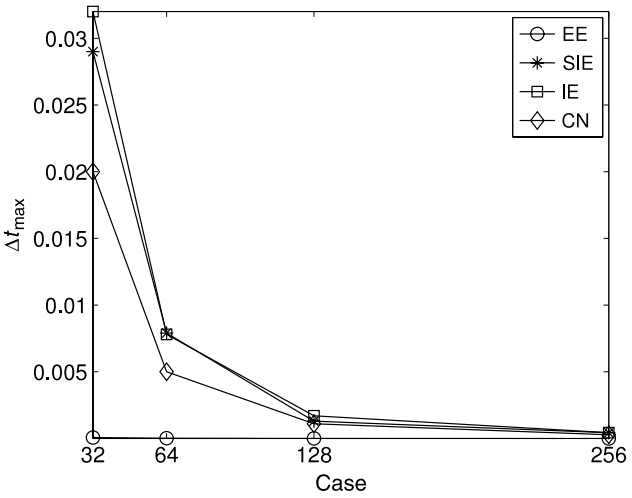

Fig. 1. The maximum time step ($\Delta t_{\max}$) guaranteeing the stability of each scheme.

Substituting (14) into (12) and letting $m_1 = m_2 = m_3 = m$ for simplicity, then, up to first order, we have

$$\frac{\partial \mathbf{c}}{\partial t} = \Delta \mathbf{c} \begin{pmatrix} \frac{18m^2-9m+1}{2} & \frac{3m(4m-1)}{2} & \frac{3m(4m-1)}{2} \\ \frac{3m(4m-1)}{2} & \frac{18m^2-9m+1}{2} & \frac{3m(4m-1)}{2} \\ \frac{3m(4m-1)}{2} & \frac{3m(4m-1)}{2} & \frac{18m^2-9m+1}{2} \end{pmatrix} - \epsilon^2 \Delta^2 \mathbf{c}. \tag{15}$$

After substituting $\mathbf{c}(x, t)$ from Eq. (13) into (15), we get

$$\begin{pmatrix} \alpha_k(t) \\ \beta_k(t) \\ \gamma_k(t) \end{pmatrix}' = \mathbf{A} \begin{pmatrix} \alpha_k(t) \\ \beta_k(t) \\ \gamma_k(t) \end{pmatrix}, \quad \mathbf{A} = \begin{pmatrix} a & b & b \\ b & a & b \\ b & b & a \end{pmatrix}, \tag{16}$$

where $'$ indicates the time derivative and

$$a = \frac{-k^2\pi^2}{2}(18m^2 - 9m + 1) - \epsilon^2 k^4 \pi^4, \qquad b = \frac{-3k^2\pi^2 m(4m-1)}{2}.$$

The eigenvalues of $\mathbf{A}$ are

$$\lambda_1 = -\frac{k^2\pi^2}{2}(42m^2 - 15m + 1 + 2\epsilon^2 k^2 \pi^2),$$
$$\lambda_2 = \lambda_3 = -\frac{k^2\pi^2}{2}(6m^2 - 6m + 1 + 2\epsilon^2 k^2 \pi^2).$$

The solution to the system of *ODE*s (16) is given by

$$\begin{pmatrix} \alpha_k(t) \\ \beta_k(t) \\ \gamma_k(t) \end{pmatrix} = \frac{\alpha_k(0) + \beta_k(0) + \gamma_k(0)}{3} \begin{pmatrix} 1 \\ 1 \\ 1 \end{pmatrix} e^{\lambda_1 t} + \frac{-\alpha_k(0) - \beta_k(0) + 2\gamma_k(0)}{3} \begin{pmatrix} -1 \\ 0 \\ 1 \end{pmatrix} e^{\lambda_2 t}$$
$$+ \frac{-\alpha_k(0) + 2\beta_k(0) - \gamma_k(0)}{3} \begin{pmatrix} -1 \\ 1 \\ 0 \end{pmatrix} e^{\lambda_2 t}.$$

In Fig. 2, we plot the evolution of the amplitudes as a function of time. The symbols '-○-', '-◇-', and '-△-' are numerical results that are compared with the theoretical values $\alpha_k(t)$ (point), $\beta_k(t)$ (star), and $\gamma_k(t)$ (plus), respectively, with the initial conditions:

$$c_1(x, 0) = 0.25 + 0.001 \cos(3\pi x), \tag{17}$$
$$c_2(x, 0) = 0.25 + 0.002 \cos(3\pi x), \tag{18}$$
$$c_3(x, 0) = 0.25 + 0.003 \cos(3\pi x). \tag{19}$$

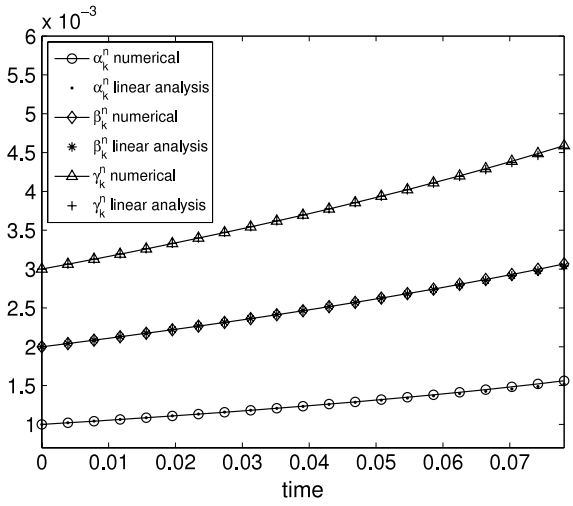

Fig. 2. The symbols '-○-', '-◇-', and '-△-' are numerical results that are compared with the theoretical values $\alpha_k(t)$ (point), $\beta_k(t)$ (star), and $\gamma_k(t)$ (plus), respectively, with the initial conditions of Eqs. (17)–(19).

Table 2
Average CPU times (s) for different numbers of components.

N	3	4	5	6	7	8	9	10
Average CPU time	2.060	2.990	4.070	5.028	5.791	6.686	7.492	8.533

Here, we used $k = 3$, $m = 0.25$, $\epsilon = 0.005$, $h = 1/256$, $\Delta t = 0.1h$, and $T = 200\Delta t$. The numerical amplitudes are defined by

$$\alpha_k^n = \left(\max_{1\le i\le N_x} c_1^n(x_i) - \min_{1\le i\le N_x} c_1^n(x_i) \right)/2,$$
$$\beta_k^n = \left(\max_{1\le i\le N_x} c_2^n(x_i) - \min_{1\le i\le N_x} c_2^n(x_i) \right)/2,$$
$$\gamma_k^n = \left(\max_{1\le i\le N_x} c_3^n(x_i) - \min_{1\le i\le N_x} c_3^n(x_i) \right)/2.$$

The results in Fig. 2 show that the linear stability analysis and numerical solutions are in good agreement in a linear regime.

4.3. The efficiency of the proposed scheme

As mentioned in Section 3.1, we can solve the N-component CH system in a decoupled way by using our scheme. In order to show the efficiency of the proposed scheme, we consider phase separation of $N = 3, 4, \ldots, 10$ components in the unit square domain $\Omega = (0, 1)\times(0, 1)$. For each number of components, the initial condition is a randomly chosen superposition of circles. We choose $h = 1/128$, $\Delta t = 10h$, and $\epsilon = 0.0047$ and perform 4000 time steps. The evolution of the interface is shown in Fig. 3. Rows 1 and 2 correspond to $t = 10\Delta t$ and $4000\Delta t$, respectively. Table 2 provides the average CPU time (in seconds) during 4000 time steps for each number of components. The average CPU time versus number of components is shown in Fig. 4. The results suggest that the convergence rate of average CPU time is linear with respect to number of components.

4.4. Spinodal decomposition—phase separation of a ten-component mixture

We consider phase separation of a ten-component mixture by spinodal decomposition. The initial condition is a randomly chosen superposition of circles. A 128×128 mesh is used on the domain $\Omega = (0, 1) \times (0, 1)$ and we take $\Delta t = 10h$ and $\epsilon = 0.0038$. We compute until the solution becomes numerically stationary. Fig. 5 shows the evolution of the interface at different times. We observe that three phases meet at one point and the angles between them approach 120° as they approach local equilibrium states. This is due to the fact that in the total energy functional equation (2), $\mathcal{F}(\mathbf{c}(\mathbf{x}, t))$ is symmetric and the interaction parameter ϵ is constant. This result is in good agreement with the theory in [66].

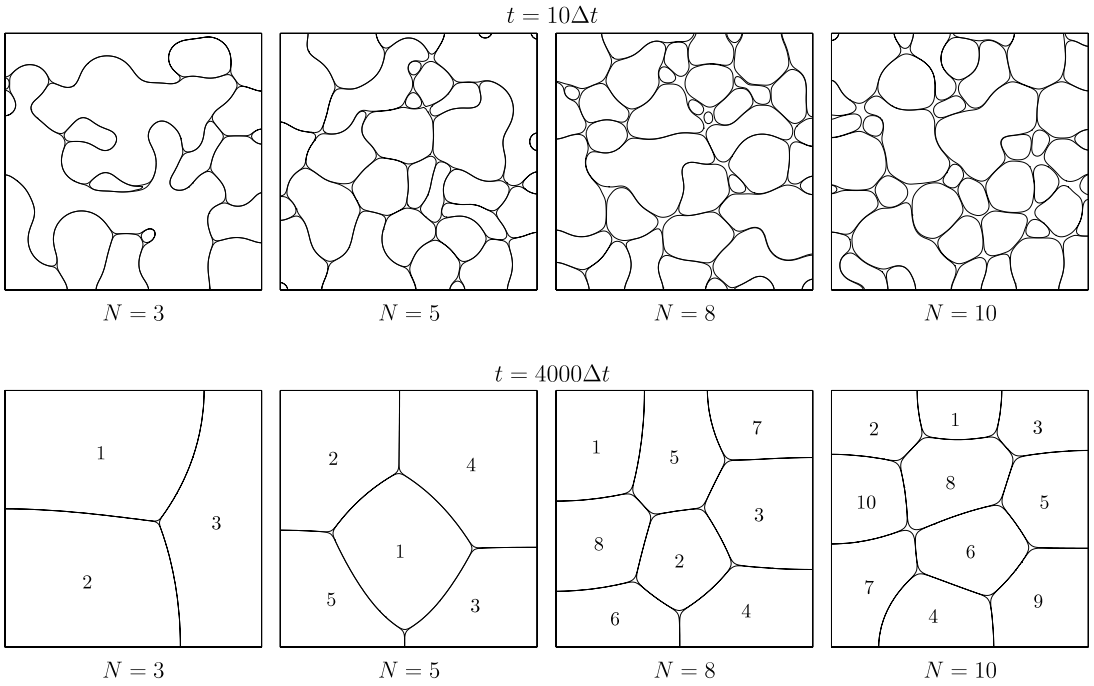

Fig. 3. Phase separation of $N = 3, 5, 8$, and 10 components. Rows 1 and 2 correspond to $t = 10\Delta t$ and $4000\Delta t$, respectively. Numbers in row 2 indicate the number of components.

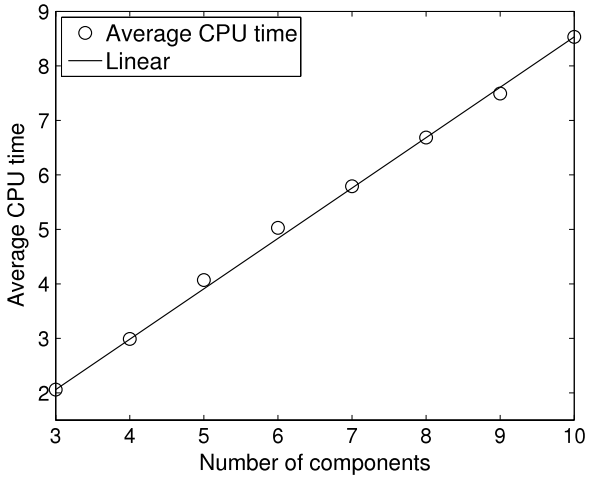

Fig. 4. Average CPU time versus number of components.

4.5. Phase separation of a five-component mixture in a gravitational field

We consider multi-component incompressible viscous fluid flow. The fluid dynamics is described by the Navier–Stokes–Cahn–Hilliard (NSCH) equations [3,7,9–13,30,46,48,56,68–70]:

$$\rho(\mathbf{c})\left(\frac{\partial \mathbf{u}}{\partial t} + \mathbf{u}\cdot\nabla\mathbf{u}\right) = -\nabla p + \eta\Delta\mathbf{u} + \rho(\mathbf{c})\mathbf{g}, \tag{20}$$

$$\nabla\cdot\mathbf{u} = 0, \tag{21}$$

$$\frac{\partial \mathbf{c}}{\partial t} + \mathbf{u}\cdot\nabla\mathbf{c} = M\Delta\boldsymbol{\mu}, \tag{22}$$

$$\boldsymbol{\mu} = \mathbf{f}(\mathbf{c}) - \epsilon^2\Delta\mathbf{c} + \beta(\mathbf{c}), \tag{23}$$

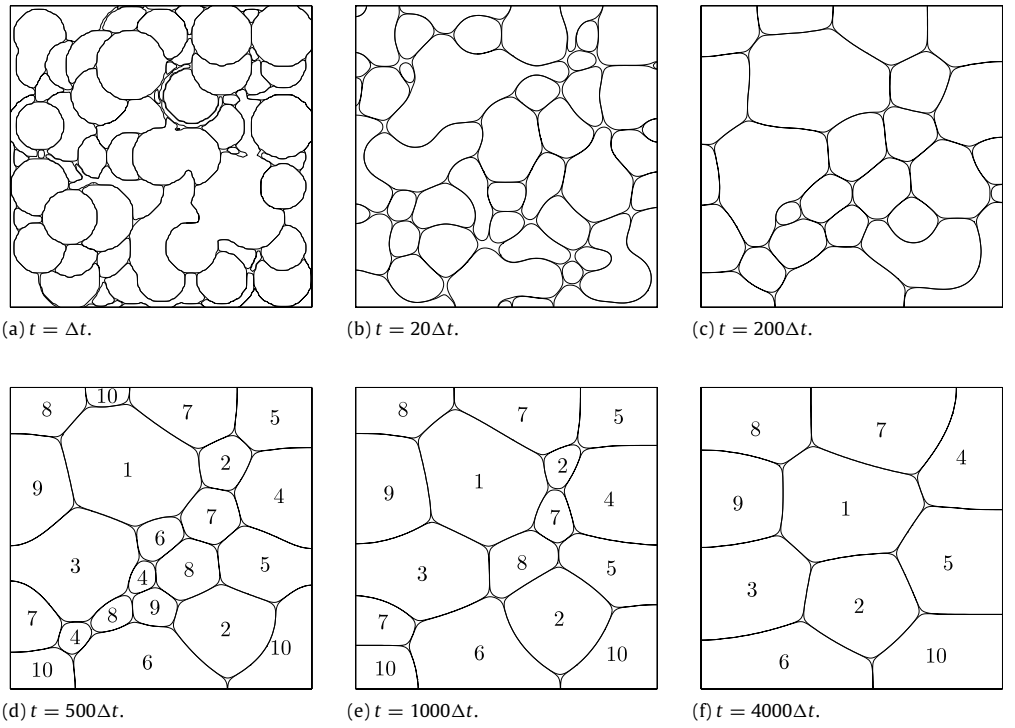

Fig. 5. Temporal evolution of a ten-component system. Times are shown below each figure. Numbers in (d), (e), and (f) indicate the number of components.

where $\mathbf{u}$ is the velocity, p is the pressure, $\rho(\mathbf{c})$ is the density, η is the viscosity, $\mathbf{g} = (0, -g)$ is the gravity, M is the mobility, and μ is the generalized chemical potential. In this paper, the effect of the surface tension is negligible. We note that even though our phase-field model can deal with a variable viscosity case straightforwardly, we focus on the viscosity matched case.

To make Eqs. (20)–(23) dimensionless, we choose the following definitions:

$$\mathbf{x}' = \frac{\mathbf{x}}{L_c}, \qquad \mathbf{u}' = \frac{\mathbf{u}}{U_c}, \qquad t' = \frac{tU_c}{L_c}, \qquad \rho' = \frac{\rho}{\rho_c}, \qquad p' = \frac{p}{\rho_c U_c^2}, \qquad \mathbf{g}' = \frac{\mathbf{g}}{g}, \qquad \boldsymbol{\mu}' = \frac{\boldsymbol{\mu}}{\mu_c},$$

where the primed quantities are dimensionless and L_c is the characteristic length, U_c is the characteristic velocity, ρ_c is the characteristic density and is defined as that of fluid 1, g is the gravitational acceleration, and μ_c is the characteristic chemical potential. Substituting these variables into Eqs. (20)–(23) and dropping the primes, we have

$$\rho(\mathbf{c})\left(\frac{\partial \mathbf{u}}{\partial t} + \mathbf{u}\cdot\nabla\mathbf{u}\right) = -\nabla p + \frac{1}{\mathrm{Re}}\Delta\mathbf{u} + \frac{\rho(\mathbf{c})}{\mathrm{Fr}^2}\mathbf{g}, \tag{24}$$

$$\nabla\cdot\mathbf{u} = 0, \tag{25}$$

$$\frac{\partial \mathbf{c}}{\partial t} + \mathbf{u}\cdot\nabla\mathbf{c} = \frac{1}{\mathrm{Pe}}\Delta\boldsymbol{\mu}, \tag{26}$$

$$\boldsymbol{\mu} = \mathbf{f}(\mathbf{c}) - \epsilon^2\Delta\mathbf{c} + \beta(\mathbf{c}), \tag{27}$$

where $\mathbf{g} = (0, -1)$ and ϵ is redefined according to the scaling. The dimensionless parameters are the Reynolds number, $\mathrm{Re} = \rho_c U_c L_c/\eta$, Froude number, $\mathrm{Fr} = U_c/\sqrt{gL_c}$, and Peclet number, $\mathrm{Pe} = U_c L_c/(M\mu_c)$. Using $U_c = \sqrt{gL_c}$, we have $\mathrm{Re} = \rho_c U_c L_c/\eta = \rho_c g^{1/2} {L_c}^{3/2}/\eta$ and $\mathrm{Fr} = U_c/\sqrt{gL_c} = \sqrt{gL_c}/\sqrt{gL_c} = 1$. By applying our scheme, we can solve the multi-component advective CH system (26) and (27) in a decoupled way and solving the multi-component NSCH system (24)–(27) becomes solving the binary NSCH system. For a detailed description of the numerical method used in solving the binary NSCH system, please refer to Ref. [13].

To model phase separation of a five-component mixture in a gravitational field, we take an initial velocity field as zero, $\mathbf{u} = \mathbf{0}$, and the initial conditions for $\mathbf{c}$ are randomly distributed between 0 and 1. $\rho(\mathbf{c}) = \sum_{i=1}^{5}\rho_i c_i$ ($c_5 = 1 - c_1 - c_2 - c_3 - c_4$ and ρ_i is the ith fluid density) and $\rho_i = 6 - i$ for $i = 1, \ldots, 5$. A mesh size 128×128 is used on the unit square domain and we choose $\Delta t = 2.0 \times 10^{-3}$, $\epsilon = 0.0047$, $\mathrm{Re} = 3000$, and $\mathrm{Pe} = 0.1/\epsilon$. Fig. 6 shows the time evolution of the five-component mixture system in a gravitational field. Fluid 1 is represented by the black region, fluid 2 by the dark gray region, fluid 3 by

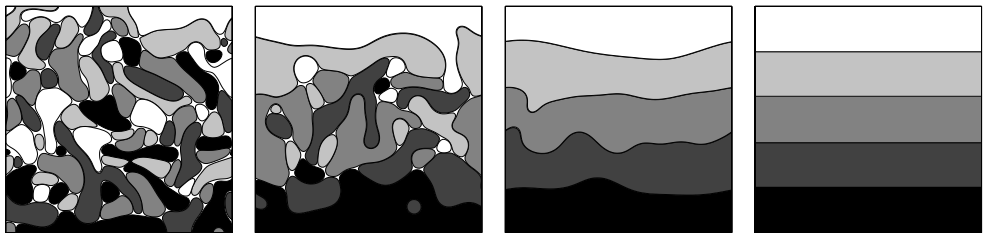

Fig. 6. Phase separation of a five-component mixture in a gravitational field. Fluid 1 is represented by the black region, fluid 2 by the dark gray region, fluid 3 by the gray region, fluid 4 by the light gray region, and fluid 5 by the white region. Times are shown below each figure.

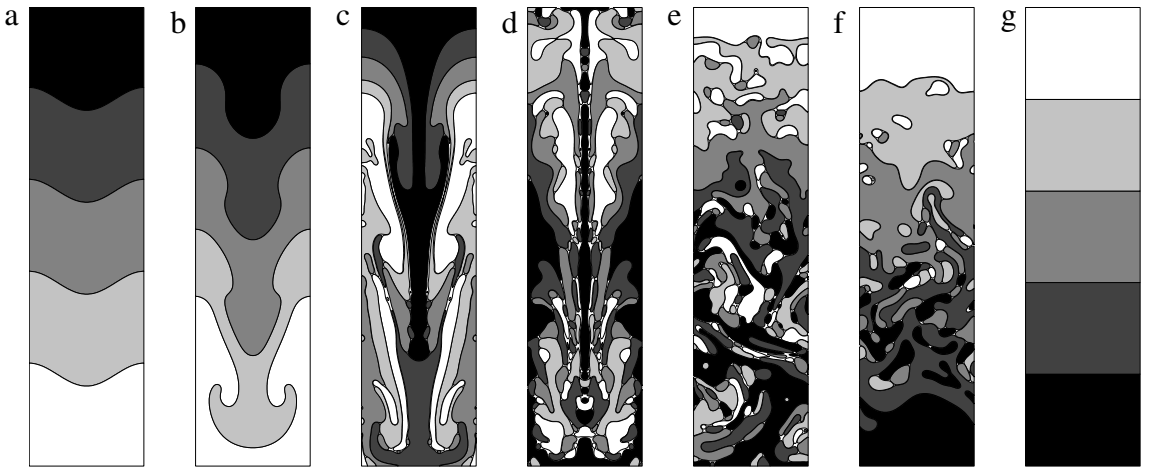

Fig. 7. The Rayleigh–Taylor instability of a five-component mixture. Times are $t = 0$, 3, 6, 10, 20, 40, and 160 (left to right).

the gray region, fluid 4 by the light gray region, and fluid 5 by the white region. From Fig. 6 we see that the gravity affects a multi-component simulation by pulling the heavy fluid to the bottom of the computational domain.

4.6. The Rayleigh–Taylor instability of a five-component mixture

When a heavy fluid is superposed over a light fluid in a gravitational field, the fluid interface is unstable. Any perturbation of this interface tends to grow with time, producing the phenomena known as the Rayleigh–Taylor instability. The phenomena are the penetration of both heavy and light fluids into each other. The Rayleigh–Taylor instability for a fluid in a gravitational field was originally introduced by Rayleigh [71] and later applied to all accelerated fluids by Taylor [72].

In this section, we study the Rayleigh–Taylor instability of a five-component mixture. In the simulations, we have two initial states as shown in Figs. 7(a) and 8(a). The initial velocity is zero. $\rho(\mathbf{c}) = \sum_{i=1}^{5} \rho_i c_i$ ($c_5 = 1 - c_1 - c_2 - c_3 - c_4$ and ρ_i is the ith fluid density) and $\rho_i = 6 - i$ for $i = 1, \ldots, 5$. A mesh size 128×512 is used on a domain $\Omega = (0, 1) \times (0, 4)$ and we choose $\Delta t = 2.0 \times 10^{-3}$, $\epsilon = 0.0047$, Re $= 3000$, and Pe $= 0.1/\epsilon$. The results are presented in Figs. 7(b)–(g) and 8(b)–(g). The area shown by black indicates the fluid 1 region, while the dark gray, gray, light gray, and white color regions stand for the fluid 2, 3, 4, and 5 domains, respectively. We observe that our proposed method is a powerful tool to simulate the Rayleigh–Taylor instability between multi-component fluids.

5. Conclusions

We presented a practically unconditionally gradient stable conservative nonlinear numerical scheme for the N-component Cahn–Hilliard system modeling the phase separation of an N-component mixture. The scheme is based on a nonlinear splitting method and is solved by an efficient and accurate nonlinear multigrid method. The scheme allows us to convert the N-component Cahn–Hilliard system into a system of $N - 1$ binary Cahn–Hilliard equations and significantly reduces the required computer memory and CPU time. We observed that our numerical solutions are consistent with the linear stability analysis results. We also demonstrated the efficiency of the proposed scheme with various numerical experiments.

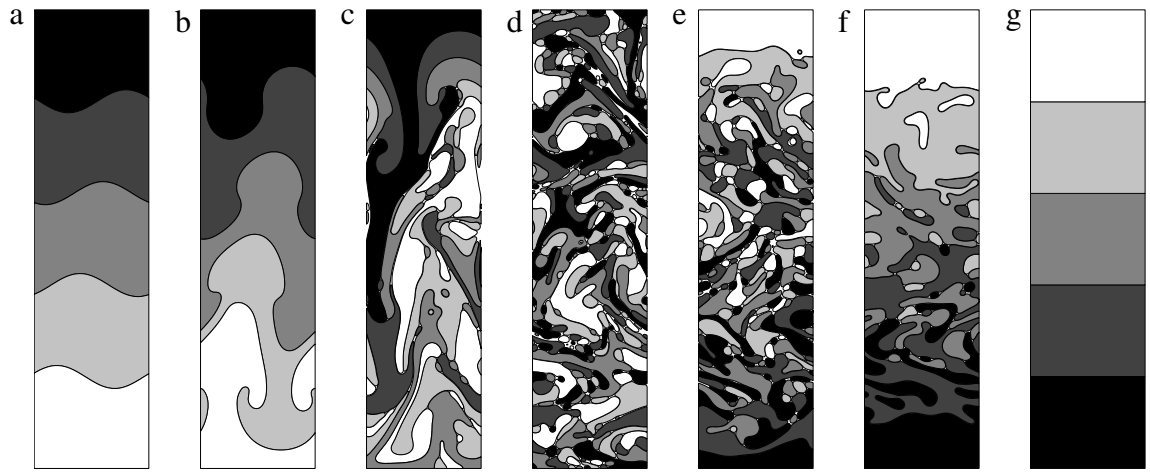

Fig. 8. The Rayleigh–Taylor instability of a five-component mixture. Times are $t = 0$, 3, 6, 10, 30, 50, and 200 (left to right).

Acknowledgment

This research was supported by Basic Science Research Program through the National Research Foundation of Korea (NRF) funded by the Ministry of Education, Science and Technology (No. 2011-0023794).

References

[1] J.W. Cahn, J.E. Hilliard, Free energy of a nonuniform system. I. Interfacial free energy, J. Chem. Phys. 28 (1958) 258–267.
[2] P. Seppecher, Moving contact lines in the Cahn–Hilliard theory, Internat. J. Engrg. Sci. 34 (1996) 977–992.
[3] D. Jacqmin, Contact-line dynamics of a diffuse fluid interface, J. Fluid Mech. 402 (2000) 57–88.
[4] H.G. Lee, J.S. Kim, Accurate contact angle boundary conditions for the Cahn–Hilliard equations, Comput. Fluids 44 (2011) 178–186.
[5] D.M. Anderson, G.B. McFadden, A diffuse-interface description of internal waves in a near-critical fluid, Phys. Fluids 9 (1997) 1870–1879.
[6] L. de Sobrino, J. Peternelj, On capillary waves in the gradient theory of interfaces, Can. J. Phys. 63 (1985) 131–134.
[7] R. Chella, J. Viñals, Mixing of a two-phase fluid by cavity flow, Phys. Rev. E 53 (1996) 3832–3840.
[8] B.T. Nadiga, S. Zaleski, Investigations of a two-phase fluid model, Eur. J. Mech. B Fluids 15 (1996) 885–896.
[9] C.H. Kim, S.H. Shin, H.G. Lee, J.S. Kim, Phase-field model for the pinchoff of liquid–liquid jets, J. Korean Phys. Soc. 55 (2009) 1451–1460.
[10] D. Jacqmin, Calculation of two-phase Navier–Stokes flows using phase-field modeling, J. Comput. Phys. 155 (1999) 96–127.
[11] H. Ding, P.D.M. Spelt, C. Shu, Diffuse interface model for incompressible two-phase flows with large density ratios, J. Comput. Phys. 226 (2007) 2078–2095.
[12] A. Celani, A. Mazzino, P. Muratore-Ginanneschi, L. Vozella, Phase-field model for the Rayleigh–Taylor instability of immiscible fluids, J. Fluid Mech. 622 (2009) 115–134.
[13] H.G. Lee, K.M. Kim, J.S. Kim, On the long time simulation of the Rayleigh–Taylor instability, Internat. J. Numer. Methods Engrg. 85 (2011) 1633–1647.
[14] S.M. Wise, J.S. Lowengrub, H.B. Frieboes, V. Cristini, Three-dimensional multispecies nonlinear tumor growth-I Model and numerical method, J. Theoret. Biol. 253 (2008) 524–543.
[15] V. Cristini, X. Li, J.S. Lowengrub, S.M. Wise, Nonlinear simulations of solid tumor growth using a mixture model: invasion and branching, J. Math. Biol. 58 (2009) 723–763.
[16] S.M. Wise, J.S. Lowengrub, V. Cristini, An adaptive multigrid algorithm for simulating solid tumor growth using mixture models, Math. Comput. Modelling 53 (2011) 1–20.
[17] D. Jasnow, J. Viñals, Coarse-grained description of thermo-capillary flow, Phys. Fluids 8 (1996) 660–669.
[18] M. Verschueren, F.N. van de Vosse, H.E.H. Meijer, Diffuse-interface modelling of thermocapillary flow instabilities in a Hele–Shaw cell, J. Fluid Mech. 434 (2001) 153–166.
[19] F. Campelo, A. Hernández-Machado, Dynamic model and stationary shapes of fluid vesicles, Eur. Phys. J. E 20 (2006) 37–45.
[20] S. Bhattacharyya, T.A. Abinandanan, A study of phase separation in ternary alloys, Bull. Mater. Sci. 26 (2003) 193–197.
[21] D. de Fontaine, A computer simulation of the evolution of coherent composition variations in solid solutions, Ph.D. Thesis, Northwestern University, 1967.
[22] J.E. Morral, J.W. Cahn, Spinodal decomposition in ternary systems, Acta Metall. 19 (1971) 1037–1045.
[23] J.J. Hoyt, The continuum theory of nucleation in multicomponent systems, Acta Metall. 38 (1990) 1405–1412.
[24] C.M. Elliott, S. Luckhaus, A generalised diffusion equation for phase separation of a multi-component mixture with interfacial free energy, IMA Preprint Series, 887, 1991.
[25] D.J. Eyre, Systems of Cahn–Hilliard equations, SIAM J. Appl. Math. 53 (1993) 1686–1712.
[26] C.M. Elliott, H. Garcke, Diffusional phase transitions in multicomponent systems with a concentration dependent mobility matrix, Physica D 109 (1997) 242–256.
[27] S. Maier-Paape, B. Stoth, T. Wanner, Spinodal decomposition for multicomponent Cahn–Hilliard systems, J. Stat. Phys. 98 (2000) 871–896.
[28] M. Honjo, Y. Saito, Numerical simulation of phase separation in Fe–Cr binary and Fe–Cr–Mo ternary alloys with use of the Cahn–Hilliard equation, ISIJ Int. 40 (2000) 914–919.
[29] J.S. Kim, K.K. Kang, J. Lowengrub, Conservative multigrid methods for Cahn–Hilliard fluids, J. Comput. Phys. 193 (2004) 511–543.
[30] J.S. Kim, A continuous surface tension force formulation for diffuse-interface models, J. Comput. Phys. 204 (2005) 784–804.
[31] J.S. Kim, A diffuse-interface model for axisymmetric immiscible two-phase flow, Appl. Math. Comput. 160 (2005) 589–606.
[32] E.V.L. de Mello, O.T. Silveira Filho, Numerical study of the Cahn–Hilliard equation in one, two and three dimensions, Physica A 347 (2005) 429–443.
[33] S. Wise, J.S. Kim, J. Lowengrub, Solving the regularized, strongly anisotropic Cahn–Hilliard equation by an adaptive nonlinear multigrid method, J. Comput. Phys. 226 (2007) 414–446.
[34] J.S. Kim, A numerical method for the Cahn–Hilliard equation with a variable mobility, Commun. Nonlinear Sci. Numer. Simul. 12 (2007) 1560–1571.

[35] Y. He, Y. Liu, Tao Tang, On large time-stepping methods for the Cahn–Hilliard equation, Appl. Numer. Math. 57 (2007) 616–628.
[36] H. Gõmez, V.M. Calo, Y. Bazilevs, T.J.R. Hughes, Isogeometric analysis of the Cahn–Hilliard phase-field model, Comput. Methods Appl. Mech. Engrg. 197 (2008) 4333–4352.
[37] L. Cueto-Felgueroso, J. Peraire, A time-adaptive finite volume method for the Cahn–Hilliard and Kuramoto–Sivashinsky equations, J. Comput. Phys. 227 (2008) 9985–10017.
[38] R.H. Stogner, G.F. Carey, B.T. Murray, Approximation of Cahn–Hilliard diffuse interface models using parallel adaptive mesh refinement and coarsening with C_1 elements, Internat. J. Numer. Methods Engrg. 76 (2008) 636–661.
[39] L.-P. He, Y. Liu, A class of stable spectral methods for the Cahn–Hilliard equation, J. Comput. Phys. 228 (2009) 5101–5110.
[40] S.D. Yang, H.G. Lee, J.S. Kim, A phase-field approach for minimizing the area of triply periodic surfaces with volume constraint, Comput. Phys. Commun. 181 (2010) 1037–1046.
[41] T. Ohta, M. Motoyama, A. Ito, The kinetics and morphology of phase-separating copolymer mixtures, J. Phys.: Condens. Matter 8 (1996) A65–A80.
[42] B.F. Barton, A.J. McHugh, Kinetics of thermally induced phase separation in ternary polymer solutions. I. Modeling of phase separation dynamics, J. Polym. Sci., Part B: Polym. Phys. 37 (1999) 1449–1460.
[43] M.I.M. Copetti, Numerical experiments of phase separation in ternary mixtures, Math. Comput. Simulation 52 (2000) 41–51.
[44] Y.Q. Ma, Domain patterns in ternary mixtures with different interfacial properties, J. Chem. Phys. 114 (2001) 3734–3738.
[45] J.S. Kim, K.K. Kang, J. Lowengrub, Conservative multigrid methods for ternary Cahn–Hilliard systems, Commun. Math. Sci. 2 (2004) 53–77.
[46] J.S. Kim, J. Lowengrub, Phase field modeling and simulation of three-phase flows, Interfaces Free Bound. 7 (2005) 435–466.
[47] P.R. Cha, D.H. Yeon, J.K. Yoon, Phase-field model for multicomponent alloy solidification, J. Cryst. Growth 274 (2005) 281–293.
[48] F. Boyer, C. Lapuerta, Study of a three component Cahn–Hilliard flow model, M2AN Math. Model. Numer. Anal. 40 (2006) 653–687.
[49] J.S. Kim, Phase field computations for ternary fluid flows, Comput. Methods Appl. Mech. Engrg. 196 (2007) 4779–4788.
[50] Y. Xia, Y. Xu, C.W. Shu, Local discontinuous Galerkin methods for the Cahn–Hilliard type equations, J. Comput. Phys. 227 (2007) 472–491.
[51] J.W. Barrett, H. Garcke, R. Nürnberg, A parametric finite element method for fourth order geometric evolution equations, J. Comput. Phys. 222 (2007) 441–467.
[52] J.S. Kim, K.K. Kang, A numerical method for the ternary Cahn–Hilliard system with a degenerate mobility, Appl. Numer. Math. 59 (2009) 1029–1042.
[53] S. Zhou, M.Y. Wang, Multimaterial structural topology optimization with a generalized Cahn–Hilliard model of multiphase transition, Struct. Multidiscip. Optim. 33 (2007) 89–111.
[54] H.G. Lee, J.S. Kim, A second-order accurate non-linear difference scheme for the N-component Cahn–Hilliard system, Physica A 387 (2008) 4787–4799.
[55] T. Kitashima, J. Wang, H. Harada, Phase-field simulation with the CALPHAD method for the microstructure evolution of multi-component Ni-base superalloys, Intermetallics 16 (2008) 239–245.
[56] J.S. Kim, A generalized continuous surface tension force formulation for phase-field models for multi-component immiscible fluid flows, Comput. Methods Appl. Mech. Engrg. 198 (2009) 3105–3112.
[57] R. Nürnberg, Numerical simulations of immiscible fluid clusters, Appl. Numer. Math. 59 (2009) 1612–1628.
[58] R. Kobayashi, J.A. Warren, W.C. Carter, A continuum model of grain boundaries, Physica D 140 (2000) 141–150.
[59] C.E. Krill III, L.-Q. Chen, Computer simulation of 3-D grain growth using a phase-field model, Acta Mater. 50 (2002) 3057–3073.
[60] J.A. Warren, R. Kobayashi, A.E. Lobkovsky, W.C. Carter, Extending phase field models of solidification to polycrystalline materials, Acta Mater. 51 (2003) 6035–6058.
[61] J. Gruber, N. Ma, Y. Wang, A.D. Rollett, G.S. Rohrer, Sparse data structure and algorithm for the phase field method, Modelling Simul. Mater. Sci. Eng. 14 (2006) 1189–1195.
[62] S. Vedantam, B.S.V. Patnaik, Efficient numerical algorithm for multiphase field simulations, Phys. Rev. E 73 (2006) 016703-1–8.
[63] H.D. Ceniceros, A.M. Roma, A nonstiff, adaptive mesh refinement-based method for the Cahn–Hilliard equation, J. Comput. Phys. 225 (2007) 1849–1862.
[64] J.S. Kim, H.-O. Bae, An unconditionally gradient stable adaptive mesh refinement for the Cahn–Hilliard equation, J. Korean Phys. Soc. 53 (2008) 672–679.
[65] D.J. Eyre, Unconditionally gradient stable time marching the Cahn–Hilliard equation, in: Computational and Mathematical Models of Microstructural Evolution, The Material Research Society, Warrendale, PA, 1998, pp. 39–46.
[66] H. Garcke, B. Nestler, B. Stoth, On anisotropic order parameter models for multi-phase systems and their sharp interface limits, Physica D 115 (1998) 87–108.
[67] U. Trottenberg, C. Oosterlee, A. Schüller, Multigrid, Academic Press, London, 2001.
[68] V.E. Badalassi, H.D. Ceniceros, S. Banerjee, Computation of multiphase systems with phase field models, J. Comput. Phys. 190 (2003) 371–397.
[69] C. Liu, J. Shen, A phase field model for the mixture of two incompressible fluids and its approximation by a Fourier-spectral method, Physica D 179 (2003) 211–228.
[70] P. Yue, J.J. Feng, C. Liu, J. Shen, A diffuse-interface method for simulating two-phase flows of complex fluids, J. Fluid Mech. 515 (2004) 293–317.
[71] L. Rayleigh, Investigation of the character of the equilibrium of an incompressible heavy fluid of variable density, Proc. Lond. Math. Soc. 14 (1883) 170–177.
[72] G. Taylor, The instability of liquid surfaces when accelerated in a direction perpendicular to their planes. I, Proc. R. Soc. A 201 (1950) 192–196.